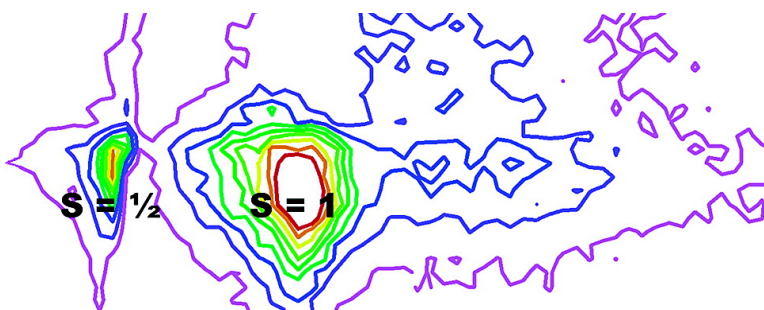


Fullerenols Revisited as Stable Radical Anions

Lars O. Husebo, Balaji Sitharaman, Ko Furukawa, Tatsuhisa Kato, and Lon J. Wilson

J. Am. Chem. Soc., **2004**, 126 (38), 12055-12064 • DOI: 10.1021/ja047593o • Publication Date (Web): 04 September 2004

Downloaded from <http://pubs.acs.org> on April 1, 2009



More About This Article

Additional resources and features associated with this article are available within the HTML version:

- Supporting Information
- Links to the 6 articles that cite this article, as of the time of this article download
- Access to high resolution figures
- Links to articles and content related to this article
- Copyright permission to reproduce figures and/or text from this article

[View the Full Text HTML](#)



Fullerenols Revisited as Stable Radical Anions

Lars O. Husebo,[†] Balaji Sitharaman,[†] Ko Furukawa,[‡] Tatsuhisa Kato,[§] and Lon J. Wilson^{*†}

Contribution from the Department of Chemistry and Center for Nanoscale Science and Technology, MS-60, Rice University, Houston, Texas 77251-1892, Institute for Molecular Science, Myodaiji, Okazaki 444-8585, Japan, and Faculty of Science, Josai University, Keyakidai 1-1, Sakado 350-0295, Japan

Received April 26, 2004; E-mail: durango@rice.edu

Abstract: The first exhaustive purification and characterization of the much-studied “fullerenols”, prepared by reaction of C₆₀ in toluene with an oxygenated, aqueous NaOH solution using tetrabutylammonium hydroxide as a phase transfer catalyst, has been performed. The resulting fullereneol is not simply polyhydroxylated C₆₀ but rather is a structurally and electronically complex C₆₀ radical anion with a molecular formula of Na⁺[C₆₀O_x(OH)_y]ⁿ⁻ (where $n = 2-3$, $x = 7-9$, and $y = 12-15$) for three different, but identical, preparations. Surprisingly, Na⁺-fullereneol is paramagnetic, exhibiting μ_B values in aqueous solution of 1.9–2.1 B.M. at 0.5 T and 300 K and R₁ proton relaxivities of 0.55–0.77 mM⁻¹s⁻¹ at 20 MHz and 40 °C, values both slightly higher than those expected for a pure S = 1/2 spin system. ESR studies (ESE-FS and 2D nutation) of frozen aqueous solutions at 1.5 and 5.0 K establish that Na⁺-fullereneol is mainly S = 1/2 with a minor, but significant, component of S = 1. Thus, this is the first report to characterize these widely studied, water-soluble fullereneols as stable radical anions. The stability of the S = 1/2 Na⁺-fullereneol radical is likely due to a highly derivatized C₆₀ surface that protects a cyclopentadienyl radical center on the fullerene.

Introduction

Fullerene materials have recently received attention for their promise in biological and medicinal applications.¹ For example, carboxylated C₆₀ derivatives are potent antioxidants and act as neuroprotectants *in vivo*,² and endohedral metallofullerenes have been suggested for use in MRI and diagnostic and therapeutic nuclear medicine.^{3,4} A fair amount of this fullerene research has involved polyhydroxylated fullerenes (fullerenols)^{5–12} and metallofullerenes (metallofullerenols).^{4,13} Fullerenols are excel-

lent free radical scavengers,¹⁴ making them efficient antioxidants that decrease oxidative stress and subsequent death of cultured cortical neurons.¹⁵ Several methods have been developed to synthesize water-soluble fullereneols. Most published methods involve the hydrolysis of a fullerene intermediate made through the use of nitronium chemistry,⁶ sulfuric and nitric acid,⁷ oleum,⁸ nitrogen dioxide radicals,⁹ or hydroboration.¹⁰ The method of polyhydroxylation in this work is by far the simplest and involves the reaction of an aqueous NaOH solution in contact with a toluene or benzene solution of C₆₀ using tetrabutylammonium hydroxide (TBAH) as a phase transfer agent.^{11,12} This method has become the method of choice for polyhydroxylation of fullerenes and metallofullerenes⁴ when only a small quantity of material is available.

[†] Rice University.[‡] Institute for Molecular Science.[§] Josai University.

- (a) Wilson, L. J. *Electrochem. Soc. Interface* **1999**, *8*, 24–28. (b) Wilson, S. R. In *Fullerenes in Chemistry, Physics, and Technology*; Kadish, K. M., Ruoff, R. S., Eds.; John Wiley & Son: New York, 2000; p 437.
- (a) Thrash, T. P.; Turetsky, D. M.; Du, C.; Lobner, D.; Wheeler, M.; Almlı, C. R.; Shen, C. K. F.; Luh, T.-Y.; Choi, D. W.; Lin, T.-S. *Proc. Natl. Acad. Sci. U.S.A.* **1997**, *94*, 9434–9439.
- (a) Wilson, L. J.; Cagle, D. W.; Thrash, T. P.; Kennel, S. J.; Mirzadeh, S.; Alford, J. M.; Ehrhardt, G. J. *Coord. Chem. Rev.* **1999**, *190–192*, 199–207. (b) Thrash, T. P.; Cagle, D. W.; Alford, J. M.; Wright, K.; Ehrhardt, G. J.; Mirzadeh, S.; Wilson, L. J. *Chem. Phys. Lett.* **1999**, *308*, 329–336. (c) Bolskar, R. D.; Benedetto, A. F.; Husebo, L. O.; Price, R. E.; Jackson, E. F.; Wallace, S.; Wilson, L. J.; Alford, J. M. *J. Am. Chem. Soc.* **2003**, *125*, 5471–5478.
- (a) Cagle, D. W.; Kennel, S. J.; Mirzadeh, S.; Alford, J. M.; Wilson, L. J. *Proc. Natl. Acad. Sci. U.S.A.* **1999**, *96*, 5182–5187. (b) Mikawa, M.; Kato, H.; Okumura, M.; Narazaki, M.; Kanazawa, Y.; Miwa, N.; Shinohara, H. *Bioconjugate Chem.* **2001**, *12*, 510–514. (c) Kato, H.; Kanazawa, Y.; Okumura, M.; Taninaka, A.; Yokawa, T.; Shinohara, H. *J. Am. Chem. Soc.* **2003**, *125*, 4391–4397.
- Naim, A.; Shevlin, P. B. *Tetrahedron Lett.* **1992**, *33*, 7097–7100.
- Chiang, L. Y.; Upasani, R. B.; Swirczewski, J. W. *J. Am. Chem. Soc.* **1992**, *114*, 10154–10157.
- (a) Chiang, L. Y.; Swirczewski, J. W.; Hsu, C. S.; Chowdhury, S. K.; Cameron, S.; Creegan, K. J. *Chem. Soc., Chem. Commun.* **1992**, 1791–1793. (b) Chiang, L. Y.; Upasani, R. B.; Swirczewski, J. W.; Soled, S. J. *Am. Chem. Soc.* **1993**, *115*, 5453–5457.

- (a) Chen, B.-H.; Huang, J.-P.; Wang, L. Y.; Shiea, J.; Chen, T.-L.; Chiang, L. Y. *J. Chem. Soc., Perkin Trans. 1* **1998**, 1171–1174. (b) Chen, B.-H.; Canteenwala, T.; Patil, S.; Chiang, L. Y. *Synth. Commun.* **2001**, *31*, 1659–1667.
- Chiang, L. Y.; Bhonsle, J. B.; Wang, L.; Shu, S. F.; Chang, T. M.; Hwu, J. R. *Tetrahedron* **1996**, *52*, 4963–4972.
- Schneider, N. S.; Darwish, A. D.; Kroto, H. W.; Taylor, R.; Walton, D. R. M. *J. Chem. Soc., Chem. Commun.* **1994**, 463–464.
- (a) Li, J.; Takeuchi, A.; Ozawa, M.; Li, X.; Saigo, K.; Kitazawa, K. *J. Chem. Soc., Chem. Commun.* **1993**, 1784–1785. (b) Li, T.; Li, X.; Huang, K.; Jiang, H.; Li, J. *J. Cent. South Univ. Technol. (Engl. Ed.)* **1999**, *6*, 35–36.
- Gonzalez, K. A.; Wilson, L. J.; Wu, W.; Nancollas, G. H. *Bioorg. Med. Chem.* **2002**, *10*, 1991–1997.
- Sun, D.; Huang, H.; Yang, S.; Liu, Z. L. S. *Chem. Mater.* **1999**, *11*, 1003–1006.
- (a) Chiang, L. Y.; Lu, F.-J.; Lin, J.-T. *J. Chem. Soc., Chem. Commun.* **1995**, 1283–1284. (b) Jeng, U. S.; Lin, T. L.; Chang, T. S.; Lee, H. Y.; Hsu, C. H.; Hsieh, Y. W.; Canteenwala, T.; Chiang, L. Y. *Prog. Colloid Polym. Sci.* **2001**, *118*, 232–237.
- Dugan, L. L.; Gabrielsen, J. K.; Yu, S. P.; Lin, T.-S.; Choi, D. W. *Neurobiol. Disease* **1996**, *3*, 129–135.

Here, we describe the synthesis and the exhaustive purification/characterization of fullereneols prepared by the $C_{60}(\text{toluene})/\text{NaOH}_{(\text{aq.})}/\text{TBAH}$ method, and for the first time, characterize these fullereneols as stable radical anions composed of a mixture of $S = 1/2$ and $S = 1$ species. This discovery calls into question the molecular and electronic nature of many, if not all, previously reported fullereneol and metallofullereneol preparations in the literature, although the acidic preparations (not explored here) may produce different products than the NaOH preparations of the current study.

Results and Discussion

Synthesis and Purification. Three batches of fullereneol (herein called Fullereneol-1, -2, and -3) were synthesized in exactly the same manner. The general method calls for dissolution of C_{60} in toluene at room temperature, followed by reaction with a concentrated aqueous metal hydroxide solution in the presence of tetrabutylammonium hydroxide (TBAH) as a phase transfer catalyst.^{11,12} The NaOH solution must also be oxygenated or open to the air, because the reaction does not occur in the absence of O_2 .¹¹ A literature method was followed^{11,12} with a few modifications to help ensure a high yield of fullereneol. For example, an especially large volume of concentrated NaOH solution was used and the reaction time was increased from 10 hours to 2 days. After 2 days, the resulting fullereneol material was purified by precipitation using methanol.¹¹ However, after many repetitions of redissolving the sample in freshwater, followed by reprecipitation with methanol (the usual literature method of purification,^{6,11}) the aqueous sample solution still exhibited $\text{pH} > 8$, indicating incomplete removal of NaOH. For this reason, an additional purification step, employing repeated size-exclusion column chromatography, was necessary until the aqueous fullereneol solution possessed a pH at or below that of the deionized water used to dissolve the sample (see Experimental Section).

Characterization. In addition to the expected IR absorption bands of fullereneol^{6,7,9} (O–H, 3380 cm^{-1} ; C=C, 1600 cm^{-1} ; C–OH, 1390 cm^{-1} ; C–O, 1055 cm^{-1}) there was also a weak and less-expected band observed at 1710 cm^{-1} , indicating the possible presence of a carbonyl group. Such carbonyl absorption bands have previously been observed for fullereneols,¹⁶ but more typically they are observed as the result of the conversion of hemiketals on the fullerene cage into carbonyl groups when acid is added to a fullereneol sample.⁷ In this work, when a HCl solution was added to the fullereneol solution the absorption band at 1710 cm^{-1} increased in intensity, and after treatment with a NaOH solution, the band returned to its initial intensity. This reversibility of the 1710 cm^{-1} band intensity has been suggested to be indicative of a hemiketal structure in fullereneols.⁷

All three fullereneol preparations of this work gave XPS spectra that had C_{1s} binding energies spread over 5.3 eV. As seen in Figure 1, assuming that the peak separation between each carbon oxidation state is in a range of 1.8 eV,⁷ the curve-fitting analysis of the fullereneol samples allowed the assignment of four different oxidation states for carbon. Additional XPS spectral data (5 figures and 10 tables) are available as Supporting Information.

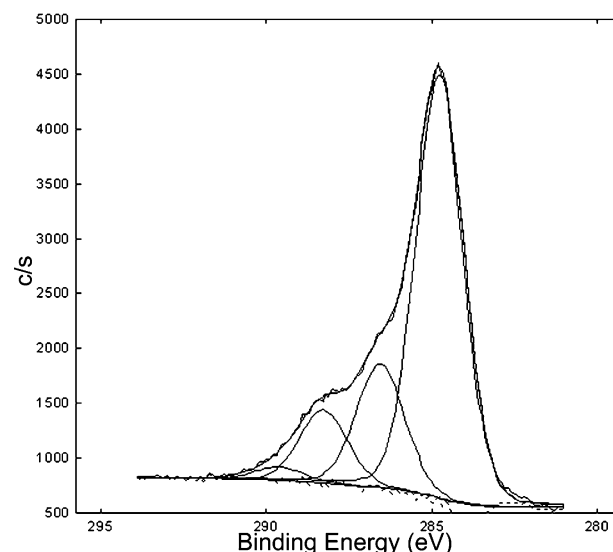


Figure 1. XPS spectrum of the C_{1s} binding energy of Fullereneol-1 and the curve-fitting analysis showing the oxidation states of carbon.

For the three fullereneol preparations of this work, we have assigned the fitted peaks with a binding energy at 284.8 eV (61–66% of total area) to nonoxygenated carbon, the peak at 286.5–286.7 eV (21–24%) to monoxygenated carbon (hydroxylated carbon), the peak at 288.3 eV (11–13%) to dioxygenated carbon (hemiketal carbon), and the peak at 289.6–290.1 eV (2%) to dioxygenated carbon (carbonyl carbon). The slightly different binding energies for the same peaks in the three different fullereneol samples is likely due to the heterogeneous composition of the fullereneol samples, as previously noted.⁷ The assignment of the two highest energy peaks to dioxygenated carbon is confirmed by the increase in area of the 290 eV peak (from 2% in the original sample to 5% in the acidified sample) and reduction in peak area of the 288 eV peak (from 13% to 9%) after treatment with HCl. The increase in the intensity of the 290 eV peak and a decrease in intensity of the 288 eV peak also support these peak assignments because a hemiketal carbon is converted into its ketone analogue by acid.

In addition to observing C_{1s} peaks (68–71%) in the fullereneol samples, O_{1s} (27–29%) and Na_{1s} (2–4%) peaks were also observed. The observation of a Na_{1s} peak could result from incomplete removal of NaOH during purification. However, after extensive size-exclusion chromatography, all the sample fractions had a pH less than that of the eluent. Typically, the fullereneol solutions of this work had a pH in the range of 5.5–6.5, and it is unlikely that NaOH remained in the sample as an impurity. Rather, it seemed more plausible that any sodium present might actually be a counterion for a fullereneol species of the type $Na^+_n[C_{60}O_x(OH)_y]^{n-}$, where n is the charge on fullereneol and x is the total number of hemiketal and carbonyl carbons on the fullerene cage. Further circumstantial evidence for a negatively charged fullereneol species was provided by the adsorption of the dark-red fullereneol solution onto an anion-exchange resin. For example, when the fullereneol solution was loaded onto an anion-exchange column, it immediately adhered to the column and would not elute, even with copious amounts of water. However, upon the addition of a saturated NaCl solution, about half the sample passed through the column immediately. This anion-exchange column behavior and the fact that the fullereneol samples formed slightly acidic solutions were

(16) Chen, Y.; Cai, R. F.; Chen, S.; Huang, Z. E. *J. Phys. Chem. Solids* **2001**, *62*, 999–1001.

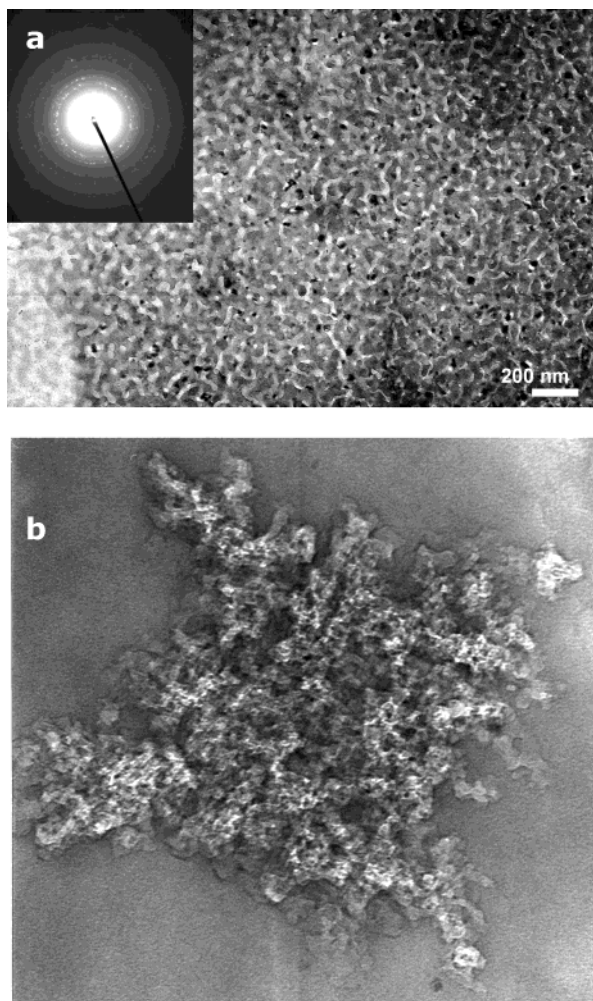


Figure 2. (a) Cryo-TEM micrograph at 155 °C of the aggregates formed by Fullereneol-1 solution microfilm (concentration = 1.8 mM, pH = 5.5). Inset shows the micro-diffraction pattern of the same microfilm; (b) TEM image of the same solution microfilm at room temperature showing the morphology of the aggregates.

the first indicators that the fullerenols of this study were, indeed, anionic in nature.

Using the relative XPS concentrations from the peak areas of C, O, and Na, in combination with the above C_{1s} curve-fitted data, it is possible to estimate the average number of hydroxyl, hemiketal, and carbonyl groups, along with a Na^+ /fullereneol ratio for each sample. In this manner, molecular formulas for the three fullereneol samples have been calculated as Fullereneol-1, $Na_2C_{60}O_8(OH)_{12}$ (MW = 1098 g mol⁻¹); Fullereneol-2, $Na_3C_{60}O_9(OH)_{15}$ (MW = 1188 g mol⁻¹); and Fullereneol-3, $Na_2C_{60}O_7(OH)_{13}$ (MW = 1099 g mol⁻¹). The number of hemiketal carbons per fullereneol molecule is 6–8, which is consistent with previous reports,⁷ and each fullereneol anion contains on average one carbonyl carbon.

To further characterize a Na^+ -fullereneol sample, we performed TEM and Cryo-TEM measurements to image the morphology of the Fullereneol-1 sample. Figure 2a displays a Cryo-TEM image obtained from an 1.8 mM aqueous solution. The image shows irregular cheesecake-like clusters homogeneously distributed. The electron-diffraction pattern shown in the inset of Figure 2a displays discrete diffracting spots, indicating a polycrystalline structure for the sample. Figure 2b is a high-magnification TEM image of the sample at room temperature

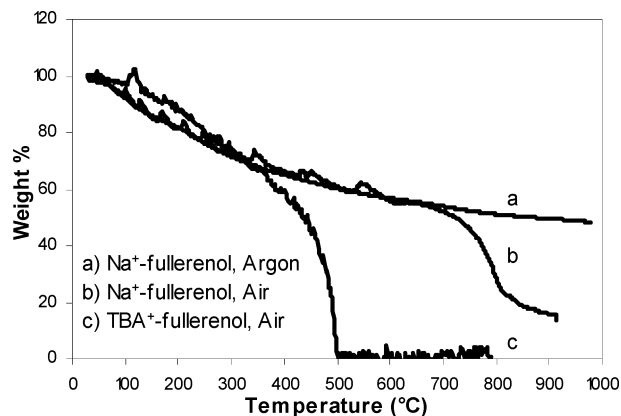


Figure 3. TGA of three fullereneol samples: (a) and (b) Na^+ form, (c) TBA^+ form. (a) Performed under argon, (b) and (c) performed under air. All are at a heating rate of 10 °C/min.

and at 1.8 mM. The sample appears as a snowflake-like structure, and as described below, this structure is thought to originate from aggregates of Na^+ -fullereneol that exist in aqueous solution at room temperature. The range of aggregate sizes has been determined by Dynamic Light Scattering (DLS) measurement, as discussed below.

Ion Exchange. The sodium ions of a fullereneol sample can be exchanged for other cations. As an example, the spectroscopic characteristics of the fullereneol sample changes upon the addition of acid (H^+). Most of the fullereneol precipitates from aqueous solution at pH < 3, and the precipitate, after several washings with an acid solution, did not contain sodium cations. In addition, conversion of hemiketal carbon to carbonyl carbon takes place, so that the molecular formula for acid-precipitated fullereneol is $C_{60}O_9(OH)_{12}$ (by XPS analysis) where the number of hemiketal carbons has been reduced from eight in Na^+ -fullereneol to six in H^+ -fullereneol and the number of carbonyl carbons has increased from one to three.

A Na^+ -fullereneol sample was also passed through a cation-exchange column loaded with tetrabutylammonium cations (TBA^+). This cation was chosen because of its nonacidic nature. For the resulting TBA^+ -fullereneol, the atomic concentrations for C (77%), O (20%), and N (2%) (by XPS analysis) indicated three TBA^+ cations per fullereneol molecule for a molecular formula of $(TBA)_3C_{60}O_8(OH)_{12}$.

The Na^+ and TBA^+ -fullereneol derivatives exhibited somewhat different properties. For example, the TBA^+ -fullereneol is much less water-soluble and the thermogravimetric analysis profile of the two compounds is significantly different (Figure 3). For Na^+ -fullereneol in air by 900 °C, 87% of the total sample mass was lost. Under argon, only 52% of the mass was lost by 1000 °C. Upon completion of these two TGA experiments, a black residue remained on each of the platinum sample pans. The black residue indicates some form of carbonaceous material and not simply sodium oxide. In contrast, for the TBA^+ -fullereneol sample in air, there is complete mass loss by 500 °C and no residue was left on the platinum pan.

In addition, for Na^+ -fullereneol, there is a steady, slow mass loss starting at room temperature and continuing to about 700 °C in air. Above 700 °C, there is a dramatic increased rate of mass loss from 700 °C to 900 °C. However, under argon the mass loss is much more gradual; it proceeds from 54% to 48% going from 700 °C to 1000 °C. The slow steady loss of sample

mass above 400 °C for both Na⁺-fullerenol samples in Figure 3 indicates that any water in the samples is lost slowly. From the TGA data alone, one cannot determine a range of temperatures in which only water is lost without loss of the Na⁺-fullerenol sample. However, the TGA data does confirm that elemental analyses (C, H, N) by combustion are invalid for these Na⁺-fullerenol samples because of the black residue that remains even at the highest temperatures. In fact, attempted elemental analyses by combustion for the Na⁺-fullerenol samples of this study resulted in only ca. 90% of the total mass being found because of incomplete combustion, even though combustion analyses have been routinely used to assign the composition of fullerenol materials in the past.^{11,16}

The anionic properties of the present fullerenol were further confirmed by solution conductivity measurements. Na⁺-Fullerenol-1 and -3 have molar conductances at 25 °C that fall between the values for 2 and 3 ions in solution (204 and 174 cm⁻¹ mol⁻¹ Ω⁻¹, respectively), while Na⁺-Fullerenol-2 has a value in the range of 3–4 ions (297 cm⁻¹ mol⁻¹ Ω⁻¹). These solution conductivity results are also consistent with the number of ions expected from the molecular formulas determined above by XPS.

Using dynamic light scattering (DLS), the aggregating properties of the fullerenol-1 sample were studied as a function of concentration, pH, and temperature. The results are tabulated (three tables) in the Supporting Information. The aggregation was found to depend little on concentration and temperature, with the mean hydrodynamic diameter being between 70 and 100 nm. However, the aggregation was found to be extremely pH sensitive for pH 3–8, with the mean hydrodynamic diameter increasing with decreasing pH and ranging between 50 and 300 nm.

SQUID Measurements. Magnetic susceptibilities of the Na⁺-fullerenols were collected as a function of temperature (2–300 K) at 0.5 T (Figure 4). Raw data (nine tables) are available as Supporting Information. The χ_M values for the Na⁺-fullerenol samples are positive at all temperatures, and the curves are those of a typical paramagnet (Figure 4a). To determine the number of unpaired electron spins, the diamagnetic contributions (calculated using an experimentally determined value for C_{60} and Pascal's constants for oxygen, hydrogen, and sodium) were subtracted from χ_M and were then used to calculate the magnetic moment, μ_B (B.M.). The range of μ_B for all the Na⁺-fullerenol samples is from 1.33 to 1.37 B.M. at 20–300 K. Comparing the experimental values of μ_B (300 K) to the theoretical spin-only magnetic moment, it is evident that the experimental values are 0.4 B.M. lower than the theoretical values for a $S = 1/2$ spin system (1.73 B.M.)

This lower value of μ_B may indicate that not all of the Na⁺-fullerenol molecules in the solid state are radicals or that some solid-state intermolecular mechanism quenches some of the paramagnetism. In fact, the sharp downturn in μ_B values below 20 K is characteristic of an intermolecular antiferromagnetic interaction. To explore this possibility, solution-state magnetic measurements were also obtained. The Na⁺-fullerenols were dissolved in water and the μ_B values were determined from 5 to 313 K. Results of the solution-state measurements are given in Figure 4a. Compared to the solid-state results, there is no apparent antiferromagnetic exchange interaction observed below 20 K. This is the expected case, because in frozen solution, each $S = 1/2$ fullerenol anion is hydrated by water molecules

and, therefore, isolated from other fullerenol anions. The μ_B values for the solution-state data are significantly higher at 300 K than for the solid state, being 1.90–2.06 B.M. at 300 K and 1.94–2.06 B.M. at 313 K. The small break in values seen between 270 and 280 K is from the phase change of water. The $\mu_{B(\text{Solution})}$ values are slightly higher than the theoretical values for a single-electron spin species, indicating that there might also be higher-spin species present in solution, and in fact, ESR studies (discussed below) demonstrate this to be the case.

The effect of acid on the paramagnetism of the fullerenol can be seen in Figure 4b, where the H⁺-fullerenol (precipitated from a solution of Na⁺-Fullerenol-2) has a positive χ_M value from 2 to 100 K, but above 100 K it becomes negative when compared to its “parent” Na⁺-fullerenol sample. However, by adding base to the H⁺-fullerenol samples, the resulting samples have solid-state χ_M values that are positive at all temperatures. The χ_M values for the fullerenol sample that precipitated from the acid solution and then were retreated with NaOH are lower than those of the original Na⁺-fullerenol. In addition, the χ_M values for the fullerenol sample that did not precipitate from the acid solution and was then retreated with NaOH, are higher than those of the original Na⁺-fullerenol. As seen in Figure 4c, in both the solid state and solution state, the fullerenol that remained in solution upon acidification superseded the “parent” fullerenol in its μ_B value after it was retreated with base, while the fullerenol that precipitated from solution did not regain the μ_B value upon retreatment with base. The acid-insoluble fullerenol, after retreatment with base, had $\mu_B = 1.74$ B.M. (300 K) in solution and $\mu_B = 1.21$ B.M. (300 K) in the solid state, while the acid-soluble fullerenol sample, after retreatment with base, showed $\mu_B = 2.71$ B.M. (300 K) in solution and 2.04 B.M. (313 K) and 2.03 B.M. (300 K) in the solid state. Thus, the “parent” fullerenol appears to separate into two Na⁺-fullerenol samples approximating $S = 1/2$ and $S = 1$ systems in solution.

ESR Measurements. The presence of both $S = 1/2$ and $S = 1$ spins in the Na⁺-fullerenol samples were confirmed by ESR measurements. A cw-ESR spectrum of Na⁺-Fullerenol-1 in frozen aqueous solution was recorded at 1.5 K by a conventional X-band spectrometer (Figure 5a). An intense broad spectrum with irregular structure was obtained around 3300 G, which corresponded to $g = 2$. The irregular structure could be due to the hyperfine interaction of a proton nuclear spin. In addition to the peak at $g = 2$, a sufficiently strong signal was observed at the half field of 1500 G, the position of $g = 4$. This signal is specific to a state of $S = 1$ or higher. Direct experimental evidence for the presence of an $S = 1$ state is given below by a two-dimensional nutation measurement. The intense signal seen at 1.5 K gradually lost intensity as the temperature was increased until it essentially disappeared by room temperature (Figure 5b). The disappearance of the signal can be attributed to fast relaxation due to the dipole interaction among the magnetizations of an $S = 1$ state. The weak signal at room temperature (Figure 5b) is in stark contrast to the only previously published ESR spectrum of a fullerenol sample.¹⁶

A two-dimensional nutation spectrum of Na⁺-Fullerenol-1 in frozen aqueous solution was measured at 5 K by a pulsed-ESR spectrometer, as shown in Figure 6a. The ordinate denotes the resonance field (gauss) ESR and the abscissa denotes the nutation frequency (MHz) at each resonance field. The vertical

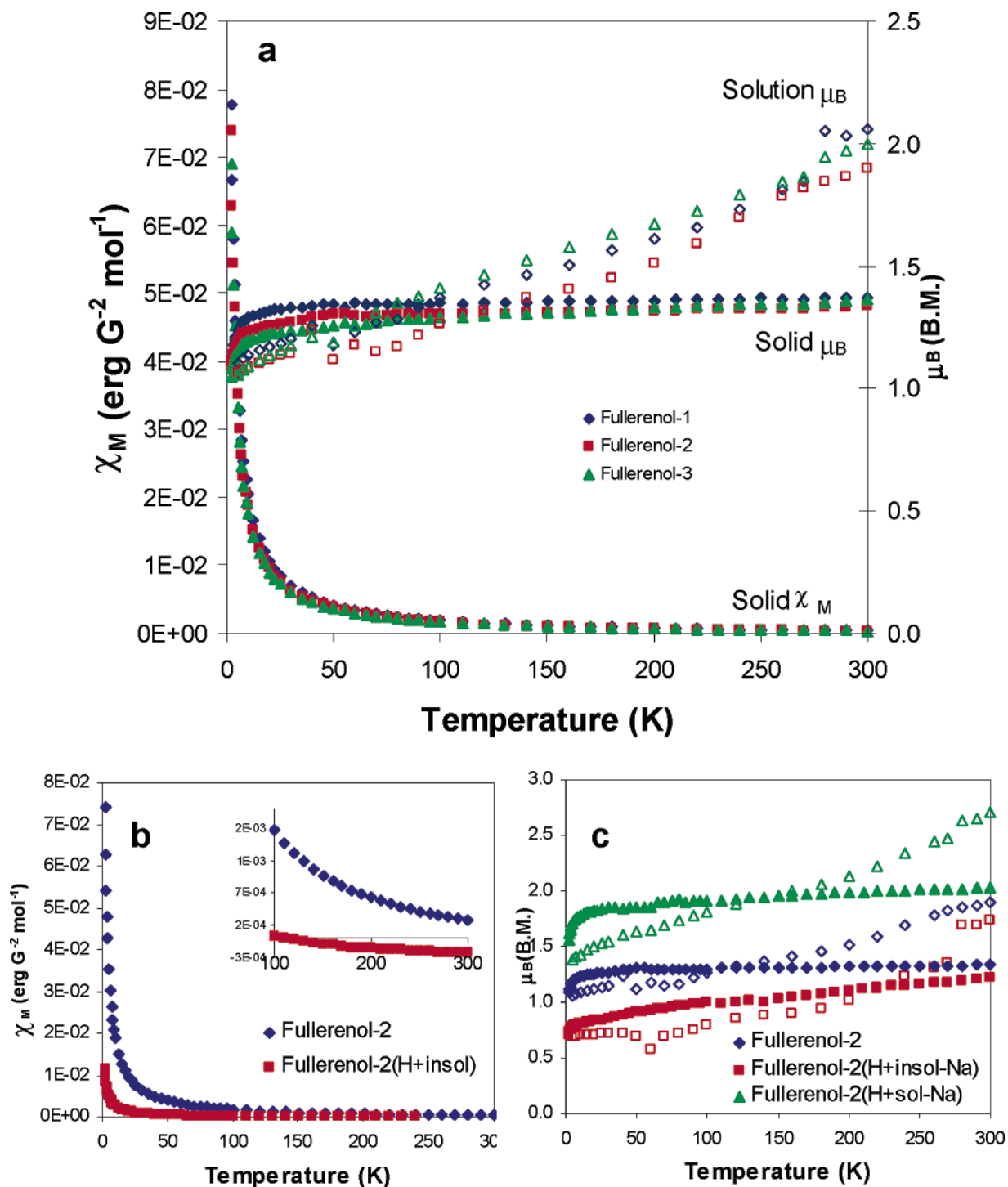


Figure 4. SQUID measurements of the Na⁺-fullerenols: (a) solid-state χ_M , and solid- and solution-state μ_B vs T of three identically prepared Na⁺-fullerenol samples; (b) solid-state χ_M vs temperature of a Na⁺-fullerenol (Fullereneol-2) before and after precipitation with acid; the inset expands the 100 to 300 K region; (c) solid- and solution-state μ_B vs T of a Na⁺-fullerenol (Fullereneol-2) after acid separation and retreatment with base. Solid symbols are for solid-state data and open symbols are for solution data.

solid line indicates the specific nutation frequency expected for each spin state of the spin-quantum number S . The monitoring nutation frequency by a pulsed-ESR spectrometer directly verifies the spin state of each component.¹⁷ The nutation frequency gives the rate of the transition in question, which is

proportional to the magnetization of the molecule determined by the spin-quantum number of S and its projection of M_s . The frequency of $S = 1/2$ is 28 MHz under the conditions of the ESR spectrometer, which should be the basic unit of the frequency $\nu_{1/2}$ as shown in Figure 6. The frequency of $S = 1$ was given as to be $\nu_{1/2}$ multiplied by the square root of 2. The observation of these frequencies is direct evidence for the spin states of $S = 1/2$ and $S = 1$. The line labeled ESEEM (electron spin-echo envelope modulation) results from the hyperfine

(17) (a) Kentgens, A. P. M.; Lemmens, J. J. M.; Geurts, F. M. M.; Veeman, W. *S. J. Magn. Reson.* **1987**, *71*, 62–74. (b) Astashkin, A. V.; Schweiger, A. *Chem. Phys. Lett.* **1990**, *174*, 595–602. (c) Takui, T.; Sato, K.; Shiomi, D.; Itoh, K.; Kaneko, T.; Tsuchida, E.; Nishide, H. *Mol. Cryst. Liq. Cryst. Sci. Technol., Sect. A* **1995**, *271*, 191–212.

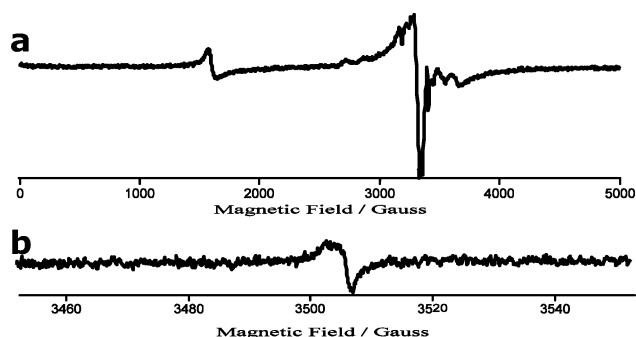


Figure 5. CW-ESR spectra of the fullerene sample (Na^+ -Fullerenol-1, 1.25 mM solution) obtained on a conventional X-band spectrometer: (a) frozen aqueous solution obtained at 1.5 K; (b) room temperature after 128 accumulated signals.

interaction with the proton nucleus of water (solvent) and does not provide information about the spin states of the fullerene sample. The intensity of the peak strongly depends on the relaxation time of a pulsed-ESR response. However, it is safe to conclude that a minor, but significant, concentration of the $S = 1$ state is observed, with the main component being fullerene with $S = 1/2$. In Figure 6b it can be seen that after three months in solution, the 2D-nutation spectrum of Na^+ -Fullerenol-1 loses most of its $S = 1/2$ signal, while the $S = 1$ signal increases significantly.

The observed presence of both the $S = 1/2$ and the $S = 1$ spin states in Na^+ -fullerenol requires some speculation. If an odd number of electrons is present on the fullerene core, a paramagnetic species of $S = 1/2$ could result. Furthermore, fullerenols with $S = 1/2$ spin may associate with each other and form “dimers” through real bonds or hydrogen bonds. If within these “dimers”, the two $S = 1/2$ centers remain unpaired, an $S = 1$ ground state could result, as indicated in the 2D nutation spectrum of Na^+ -Fullerenol-1 in Figure 6a. Such a system, where the $S = 1/2$ centers remain unpaired, is observed in the anions of $\text{C}_{120}\text{O}^{n-}$ where nutation spectra have also shown that each fullerene has an $S = 1/2$ spin, with the resulting “dimer” having an $S = 1$ spin state.¹⁸

ESR measurements were also performed on the acid-separated fullerenols (after retreatment with NaOH) to see if the difference in bulk magnetic properties in the acid-soluble and acid-insoluble fullerene products could be explained by an increase of triplet-state fullerene in the acid-soluble sample (which exhibited a high μ_B value) as compared to the acid-insoluble sample (which exhibited a lower μ_B value). As seen in Figures 5c and d, both fullerenols exhibited the strong signals of $S = 1/2$ and the broad and weak signal of $S = 1$. The differences between the two samples are (1) the fine structure of the intense peak of $S = 1/2$ for the acid-soluble Na^+ -fullerenol sample exhibited a more intense peak with more fine structure than the acid-insoluble Na^+ -fullerenol sample and (2) the acid-soluble Na^+ -fullerenol sample gave greater intensity for the half-field signal, indicating more $S = 1$ state present in the acid-soluble fraction than in the acid-insoluble fraction. This ESR result helps explain the observed bulk magnetic properties measured both in the solid and solution states for these two samples. Both the $S = 1/2$ and the $S = 1$ spin states are present in each sample, but the

Table 1. Relaxivity Values of the Three Fullerene Samples^a

compound	R_1 ($\text{mM}^{-1}\text{s}^{-1}$)	R^2
Fullerenol-1	0.77	0.99954
Fullerenol-2	0.59	0.99984
Fullerenol-3	0.55	0.99975

^a Included are the R^2 values of the linear-least-squares regression analysis.

sample with a higher magnetic moment (acid-soluble Na^+ -fullerenol) contains more $S = 1$.

Proton Relaxivity Measurements. Proton relaxivity measures the ability of a fixed concentration of a paramagnetic material to decrease the relaxation time (T_1) of protons in surrounding water.¹⁹ This ability to decrease relaxation time is used in Magnetic Resonance Imaging (MRI). In MRI, a paramagnetic, superparamagnetic, or ferromagnetic MRI contrast agent is administered to a subject, and in tissues where the contrast agent is present the relaxation times will be shortened. This will provide contrast to tissue where no contrast agent is present. In fact, the Na^+ -fullerenol material of this study has been patented as a metal-free MRI contrast agent.²⁰

Figure 7 shows the results of T_1 measurements for the three Na^+ -fullerenol samples. The data for each sample has been plotted as T_1^{-1} (s^{-1}) vs concentration (mM) and fitted by the linear-least-squares method, and the proton relaxivity (or relaxation rate (R_1)) determined from the slope of the line ($\text{mM}^{-1}\text{s}^{-1}$). The R_1 values obtained by linear least-squares regression fit can be found in Table 1.

The range of R_1 values for the three fullerenols are between $0.55\text{ mM}^{-1}\text{s}^{-1}$ and $0.77\text{ mM}^{-1}\text{s}^{-1}$, which is comparable, for example, to the relaxivity of single-electron radicals such as nitrous oxide.²¹ The effect of pH on the T_1 time can be seen in Figure 8 for Fullerene-2.

With Fullerene-2 dissolved in water (17.5 mg in 2 mL), an ambient pH of 6.7 was measured and a T_1 proton relaxation time of 0.24 s was observed. Lowering the pH to 3.2 with one drop of a 1 M HCl solution increased T_1 slightly. Upon addition of a second drop of a 12 M HCl solution, which decreased the pH to 1.4, partial precipitation occurred and T_1 increased to 1.1 s. This acid dependency is reversible, because upon increasing the pH to 6.2 (with solid NaOH), the observed T_1 decreased to near the original value before acid addition. The T_1 proton relaxation time does not further decrease with base, even with $\text{pH} > 12$ where partial precipitation occurs. Therefore, R_1 is strongly decreased in the presence of acid but not in the presence of base. Relaxation measurements were also performed on the acid-separated Na^+ -fullerenol samples, which formed the acid-soluble and acid-insoluble H^+ -fullerenol samples.

Compared to the parent Fullerene-2 sample, the acid-insoluble H^+ -fullerenol fraction appeared less soluble in water upon removal of excess acid, and it had a very small relaxivity ($0.023\text{ mM}^{-1}\text{s}^{-1}$). However, the acid-soluble H^+ -fullerenol fraction was much more soluble in water after removal of acid (under vacuum with gentle heating), and it gave a relaxivity of $0.21\text{ mM}^{-1}\text{s}^{-1}$. Acid treatment thus produces two magnetically distinct species, one that provides essentially a relaxivity of nearly zero and one that produces a measurably greater

(18) Drew, S. C.; Boas, J. F.; Pilbrow, J. R.; Boyd, P. D. W.; Paul, P.; Reed, C. A. *J. Phys. Chem. B* **2003**, *107*, 11353–11359.

(19) Hendrick, R. E.; Haacke, E. M. *J. Magn. Reson. Imaging* **1993**, *3*, 137–148.

(20) (a) Alford, J. M.; Wilson, L. J. World Patent 0124696, 2001. (b) Alford, J. M.; Wilson, L. J. U.S. Patent 6,355,225, 2002.

(21) Polnaszek, C. F.; Bryant, R. G. *J. Chem. Phys.* **1984**, *81*, 4038–4045.

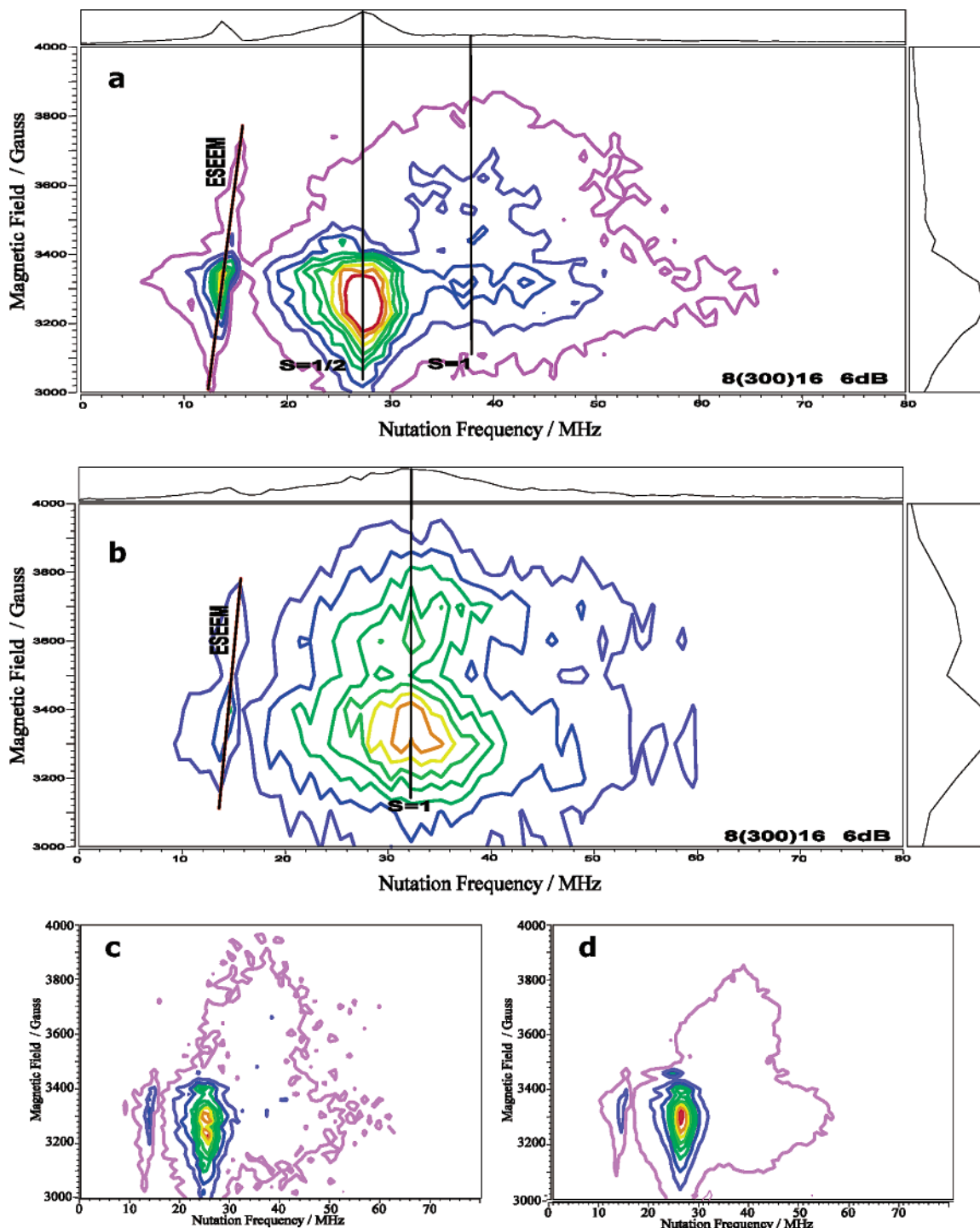


Figure 6. Two-dimensional nutation spectra in frozen aqueous solutions (1.25 mM) measured at 5 K by a pulsed-ESR spectrometer. The ordinate denotes the resonance field (gauss) ESR and the abscissa denotes the nutation frequency (MHz) at each resonance field. (a) Na⁺-Fullerenol-1; (b) three-month-old solution of (a); (c) acid-soluble fullereneol after retreatment with NaOH; (d) acid-insoluble fullereneol after retreatment with NaOH.

relaxivity. Figure 8 shows that the T_1 relaxation time decreased to the original value after the addition of base to the acidified solution, thereby increasing the relaxivity. The two acidified species of Fullereneol-2 were then separately retreated with base, and the R_1 relaxivity was again measured. In both cases the relaxivity of the base-retreated fractions increased considerably. The acid-insoluble fraction again became paramagnetic with a relaxivity of $0.30 \text{ mM}^{-1}\text{s}^{-1}$, while the acid-soluble fraction exceeded the value found for the original “parent” Fullereneol-2

by more than $0.4 \text{ mM}^{-1}\text{s}^{-1}$ to reach a value of $1.06 \text{ mM}^{-1}\text{s}^{-1}$. Thus, the “parent” Fullereneol-2 contains at least two significantly different paramagnetic species with different magnetic properties, ESR spectra, and relaxivities. These different fullereneol species possess different solubilities in acid, making clean separation of the higher- and lower-relaxivity fractions possible.

Origin of the Radical Anion. The fullerenols in this work are the first fullereneol paramagnetic anions to be reported except for an incompletely-characterized fullereneol synthesized via a

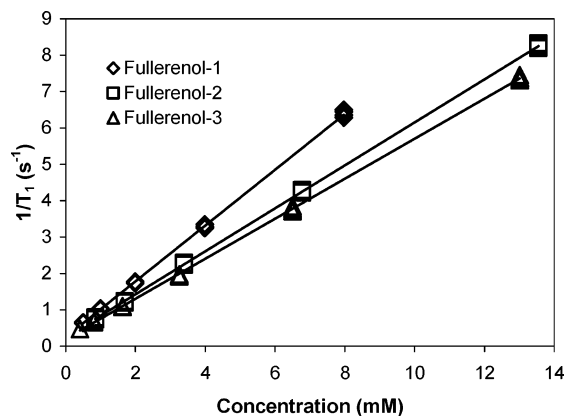


Figure 7. $1/T_1$ vs concentration of the three fullereneol samples.

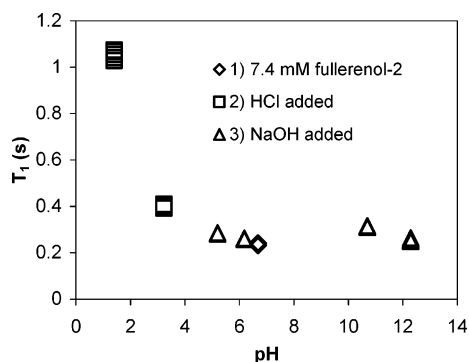
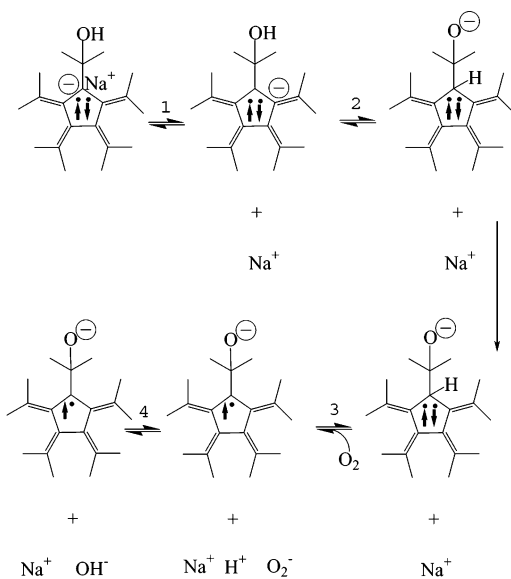


Figure 8. T_1 proton relaxation time vs pH for 7.4 mM fullereneol-2 in water.

Scheme 1



C₆₀⁻ precursor.¹⁶ The formation of the present fullereneols occurs only in the presence of molecular oxygen.¹¹ Therefore, oxygen plays an important role in the synthesis of the radical anion.

A proposed scheme for the formation of a fullereneol radical anion center is seen in Scheme 1. The starting point in the scheme is a hydroxylated fullerene carbon atom adjacent to an anionic carbon, ion-paired with a sodium cation. In step 1, the sodium cation dissociates from the carbon anion site in solution, followed by proton migration in step 2. In step 3, the carbon atom is oxidized by oxygen in air, forming a radical center on the fullerene. The O₂⁻ is short-lived and NaOH is ultimately

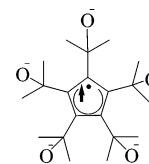


Figure 9. Fullereneol cyclopentadienyl radical anion center.

produced. If this process is repeated four more times at the neighboring carbon sites, a stable cyclopentadienyl radical could be formed as seen in Figure 9. During the formation of a “dimerized” species (through covalent or hydrogen bonding) of the paramagnetic fullereneol containing an $S = 1/2$ cyclopentadienyl radical center, electrons of the two centers would not likely become paired, and an $S = 1$ fullereneol radical “dimer” would result. The heavily derivatized fullerene surface could then protect the radical centers of the fullereneol monomers and “dimers”, to give them unusual stability in water and air.

Formation of similar cyclopentadienyl radical centers on C₆₀ have been reported in the literature. Reacting benzyl radicals with C₆₀ gives a stable cyclopentadienyl radical that is also observed in the ESR spectrum.²² In addition, these radicals can be formed by reducing C₆₀Ph₅H to the cyclopentadienyl radical, C₆₀Ph₅[•].²³ While Figure 9 shows the fullereneols of this study to be anionic by way of deprotonated hydroxyl groups, they might also be anionic by way of cyclopentadienide centers as is the case for some other literature examples.²³ In Scheme 1, atmospheric oxygen is the oxidizing agent that forms the radical. However, it is possible that other oxidizing agents (e.g., MnO₄⁻) could perform the same role.

Whatever the mechanistic details are for the formation of the fullereneol radical anions, it is now clear that “fullereneols” can be structurally and electrically complex species. Fullereneols hold a special place in fullerene chemistry because they were among the first C₆₀ derivatives to be water-solublized and studied with biological and medical purposes in mind. For these purposes, the identity and purity of materials is of paramount importance, especially for cell culture or animal testing. The fact that the present radical anions have escaped characterization or even detection for a decade is unsettling. In fact, it questions the nature of any fullereneol or metallofullereneol species in the literature and suggests that many previous studies and their results may need to be reconsidered, if it can be established that all the fullereneol syntheses in the literature give the same reaction product(s) as the present study. This question will be the subject of a future study.

Experimental Section

General. C₆₀ (99.5+%) was purchased from MER Corp. All other chemicals were purchased from Fisher Scientific except for tetrabutylammonium hydroxide (40 wt % solution in water), which was purchased from Aldrich. All chemicals were used as received. Infrared spectroscopy was performed with a Perkin-Elmer Paragon 1000 PC spectrometer. X-ray photoelectron spectroscopy (XPS) measurements were carried out using a Physical Electronics 5700 XPS spectrometer and Al K α irradiation. Thermogravimetric analyses (TGA) were performed on a Seiko 1 TG/DTA 200 instrument using platinum pans in air or

(22) Krusic, P. J.; Wasserman, E.; Keizer, P. N.; Morton, J. R.; Preston, K. F. *Science* **1991**, *254*, 1183–1185.

(23) Ikura, H.; Mori, S.; Sawamura, M.; Nakamura, E. *J. Org. Chem.* **1997**, *62*, 7912–7913.

argon and a temperature ramp of 10 °C/min. Solution conductivity measurements were performed using an YSI Model 31 conductivity bridge.

Na⁺-Fullerenol Synthesis. Three batches of fullerenols (Fullerenol-1, -2, and -3) were prepared in exactly the same manner, using a slightly modified literature procedure.^{11,12} C₆₀ (0.36 g, 0.50 mmol) was dissolved in toluene (400 mL) and sonicated until completely dissolved. The purple solution was then stirred vigorously in contact with an aqueous, concentrated sodium hydroxide solution (220.0 g NaOH in 400 mL deionized water) and 1.0 mL of tetrabutylammonium hydroxide (TBAH) as a phase-transfer catalyst. Discoloration of the toluene layer occurred within minutes. After 30 min, the stirring was stopped and the water and toluene phases were allowed to settle to form a black semisolid solution at the water/toluene interface. The nearly colorless toluene layer was then carefully removed by decantation and the remaining aqueous layer was stirred vigorously under an air sparge at room temperature for 2 days. Methanol (600 mL) was then added to the reaction flask, resulting in precipitation of the C₆₀ material and excess sodium hydroxide. The mixture of brown and white precipitate was collected by filtration on a fine fritted-glass filter and washed with 300 mL methanol. The solid was redissolved in a minimal amount of room-temperature deionized water and the resulting solution was then filtered before the addition of MeOH once again to force precipitation. This procedure was repeated a third and a fourth time. After the final filtration, the filtrate was concentrated under reduced pressure with gentle warming to a total volume of about 5 mL.

Na⁺-Fullerenol Purification. The fullerenol sample from above was split into two equal fractions and each fraction was chromatographed in water on Sephadex G-25 (fine, 20–80 μ, Aldrich) size-exclusion gel. The packed column measured 2.5" in diameter and contained 50 g (dry weight) of resin. Seven fractions were collected and the pH measured. The first fraction typically had a pH of 6.7 and the last fraction a pH of 9.9. The most basic fraction was discarded and the next three most basic fractions were then reduced in volume under vacuum with gentle heating and passed through the Sephadex column and the sample again collected in fractions. The pH of these fractions typically ranged from a pH of 6.5 to a pH of 8.5. All the fractions, except the most basic one, were then combined with the previous first fractions and the mixture was concentrated to 5 mL. This chromatography process was repeated two additional times until all the fractions off the column gave a pH at or below that of the deionized water, indicating total removal of NaOH. The fractions were then combined and concentrated under reduced pressure and gentle heating to a volume of 5 mL. The concentrated solution was then pipetted into a weighed vial. Filtered air was blown gently into the vial to evaporate the water, giving dark needlelike crystals (Fullerenol-1: 240 mg/yield: 60%, Fullerenol-2: 300 mg/yield: 70%, Fullerenol-3: 270 mg/yield 69%). UV-vis: No absorption peak maxima were observed in the visible range, however an apparent peak maximum occurred at ca. 240 nm. FTIR, KBr matrix: O–H, 3380 cm⁻¹; C=O, 1710 cm⁻¹; C=C, 1600 cm⁻¹; C–OH, 1390 cm⁻¹; C–O, 1055 cm⁻¹.

Conversion of Na⁺-Fullerenol to TBA⁺-Fullerenol. The tetrabutylammonium (TBA⁺) salt analogue of Na⁺-fullerenol was prepared by passing an aqueous sample of Fullerenol-1 through a cation-exchange resin (Dowex 50Wx8, Acros Organics) column loaded in the TBA⁺ form. Complete removal of sodium from the final TBA⁺-fullerenol sample was initially indicated by a negative sodium flame test and subsequently by XPS.

Conversion of Na⁺-Fullerenol to H⁺-Fullerenol. The protonated samples of fullerenol were prepared by adding hydrochloric acid (1 mL, 12 M) to a solution of Fullerenol-2 (51.2 mg in 5 mL water) in a centrifuge tube. A dark-colored precipitate formed immediately upon addition of acid. Upon centrifugation, an orange-red solution remained above the precipitate. The highly acidic solution was collected by decantation and the water was removed under vacuum with gentle heating until a solid formed. The sample was labeled Fullerenol-2(H⁺-

sol) and saved. The precipitate that formed upon the addition of acid to Fullerenol-2 was washed by adding 1 M HCl, then agitating, centrifuging, and decanting the slightly yellow solution two more times. The precipitate was then placed on a fine fritted-glass filter and washed with about 10 mL 1 M HCl solution (a slight yellow tint could be seen in the acid wash exiting the funnel). The precipitate was collected by adding a small amount of deionized water to the solid to dissolve the sample. The water was removed under vacuum with gentle heating until a dark crystalline solid formed. The solid was labeled Fullerenol-2(H⁺insol).

Conversion of H⁺-Fullerenol Back to Na⁺-Fullerenol. The two protonated fullerenol samples were retreated with base by dissolving the samples (either Fullerenol-2(H⁺sol) or Fullerenol-2(H⁺insol)) in water with 2 g NaOH and left to stir for 2 h. To the solution, MeOH was added to precipitate the sample, followed by collection by filtration on a fine fritted-glass funnel. The sample was then redissolved in a minimum amount of water and precipitated again with methanol, followed by filtration, dissolution, and precipitation two additional times. Due to the small quantities of sample, Fullerenol-2(H⁺sol-Na) and Fullerenol-2(H⁺insol-Na) were not chromatographed and must therefore contain small amounts of NaOH.

SQUID Measurements. Magnetic susceptibilities were measured as a function of temperature at a magnetic field of 0.5 T using a MPMS-5S SQUID magnetometer (Quantum Design) with MPMS data collection software version 2.26.2. Magnetic properties were measured on the solid samples in two 5 mm quartz ESR tubes (Wilmad) fused end-to-end, with a small vent hole on the sample side for system purging. The diamagnetic correction for the empty sample holder was determined under identical conditions as that of the sample. Solution-state measurements were performed in a 0.5 mL quartz sample holder, using a 0.4 mL solution per measurement.

ESR Measurements. The cw-ESR spectra were measured at 1.5 K by a conventional ESR spectrometer (Bruker ESP300E). Electron spin-echo detected field-scan (ESE-FS) and 2D-Nutation spectra were recorded at 5.0 K by a Bruker E680 spectrometer with Oxford Instruments cryogenics.

Relaxivity Measurements. The R₁ relaxivity measurements in aqueous solution were obtained using an IBM PC/20 MiniSpec Relaxometer operating at 40 °C and a fixed field of 0.47 T (20 MHz).

DLS Measurements. The fullerenol sample solutions were prepared by the weighing method. In all the experiments, HPLC-grade water was used and was filtered through a 0.22-μm syringe filter (Millipore, MILLEX-GP). The solutions were prepared by ultrasonication, followed by centrifugation and decantation. In some cases, the solutions were also prepared by keeping the solid in the solvent overnight and collecting the supernatant solution after centrifugation and decantation. The decanted solutions were then filtered through a 0.45-mm syringe filter (Whatman). Prior to sample loading, appropriate quartz cuvettes were cleaned with soap solution followed by rinsing with ethanol, acetone, and finally distilled water before being dried in a vacuum oven.

Measurements were performed using a Malvern Instruments Model CGS-3 multi-angle light-scattering spectrometer equipped with a multi-τ digital correlator (ALV-5000/EPP). A HeNe laser operating at a wavelength of λ_o = 632.8 nm was used as the light source with an output power of 22 mW. The scattering angle was fixed at 90° and the temperature was ranged between 15 and 55 °C. The data analysis and computation of size distribution were performed using the CONTIN routine, a constrained regularization method program for the inverse Laplace transformation of the dynamic light scattering data. The average aggregate radius and the polydispersity index (PDI) were determined by employing a second-order cumulant fit to the scattering data.

TEM Measurements. Cryo-TEM and TEM imaging were carried out on a JEOL 2000 FX electron microscope equipped with a cryogenic, heating, and tensional sample holder operating at 130 kV. Samples for the Cryo-TEM studies were prepared by dipping a copper grid coated with amorphous carbon-hole film into the sample solution. The grid

was then frozen in liquid nitrogen and immediately moved into the TEM cold stage, inserted into the column of the microscope and kept at $-155\text{ }^{\circ}\text{C}$. Precautions were taken to minimize the heating and irradiation influence of the electron beam on the samples.

Acknowledgment. L.J.W. thanks the NIH (Grant 1-R01-EB000703) and the Robert A. Welch Foundation (Grant C-0627) for support. L.O.H. also thanks the Research Council of Norway

for a graduate student fellowship.

Supporting Information Available: XPS spectra, atomic concentration tables, dynamic light scattering data tables, and tables of magnetic data. This material is available free of charge via the Internet at <http://pubs.acs.org>.

JA047593O